HHS Public Access

Author manuscript

Anal Chem. Author manuscript; available in PMC 2016 December 18.

Published in final edited form as:

Anal Chem. 2016 May 17; 88(10): 5290–5298. doi:10.1021/acs.analchem.6b00518.

Ion Mobility-Mass Spectrometry Analysis of Crosslinked Intact Multiprotein Complexes: Enhanced Gas-phase Stabilities and Altered Dissociation Pathways

Billy M. Samulak[1,2,4], **Shuai Niu**[1,5], **Philip C. Andrews**[1,2,3,*], and **Brandon T. Ruotolo**[1,*]

[1]Department of Chemistry, University of Michigan, Ann Arbor, MI 48109

[2]Department of Biological Chemistry, University of Michigan, Ann Arbor, MI 48109

[3]Department of Computational Medicine and Bioinformatics, University of Michigan, Ann Arbor, MI 48109

Abstract

Analysis of protein complexes by ion mobility-mass spectrometry is a valuable method for the rapid assessment of complex composition, binding stoichiometries, and structures. However, capturing labile, unknown protein assemblies directly from cells remains a challenge for the technology. Furthermore, ion mobility-mass spectrometry measurements of complexes, subcomplexes, and subunits are necessary to build complete models of intact assemblies, and such data can be difficult to acquire in a comprehensive fashion. Here, we present the use of novel mass spectrometry cleavable crosslinkers and tags to stabilize intact protein complexes for ion mobility-mass spectrometry. Our data reveal that tags and linkers bearing permanent charges are superior stabilizers relative to neutral crosslinkers, especially in the context of retaining compact forms of the assembly under a wide array of activating conditions. In addition, when cross-linked protein complexes are collisionally activated in the gas-phase, a larger proportion of the product ions produced are often more compact and reflect native protein sub-complexes when compared with unmodified complexes activated in the same fashion, greatly enabling applications in structural biology.

Graphical Abstract

[*]**Corresponding Authors:** andrewsp@umich.edu, bruotolo@umich.edu.

[4]Current Address: Department of Chemistry & Biology, Fitchburg State University, 160 Pearl St., Fitchburg MA 01420-2697

[5]Current Address: Mylan Pharmaceuticals Inc., 781 Chestnut Ridge Rd, Morgantown, WV 26505

Supporting Information

Detailed Methods, mass spectra of all crosslinked and tagged proteins (S-1), drift-time versus m/z plots of unmodified and DC4-crosslinked avidin (S2), SDS-PAGE of select crosslinked and tagged proteins (S3), graphs comparing percentages of marker ions produced compared to oligomeric dissociation (S4), and a table of crosslinked residues observed during bottom-up analysis of avidin are included.

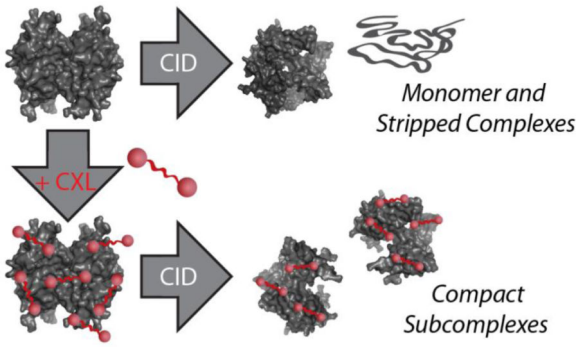

Introduction

While many critical cellular functions are carried out by proteins, few act in isolation, instead forming large macromolecular complexes[1,2]. The modular nature of many protein complexes has been revealed by a host of analytical tools[3–5], with many proteins transiently participating in multiple protein complexes. While the prevalence of transient protein complexes in cellular biology necessitates a systems biology perspective to understand functional outcomes, current knowledge bases lack many of the functional annotations necessary to accurately predict the roles of nodes and clusters within a given interaction network. This is often in part due to the absence of quantified temporal data, as well as limited information on the architecture of the complexes. Clear structural assignments of the functional protein complexes that exist within larger protein networks represent a key challenge for systems biology, and will undoubtedly require the integration of many information streams for continued progress[6,7].

Mass spectrometry (MS) based techniques have been used for decades to identify proteins from complex mixtures[8–10]. Large scale studies have been completed to identify and quantify proteins in yeast[11,12], globally map post-translational modifications[13], and to generate very rough draft maps of the human proteome[14,15]. Numerous affinity purification experiments followed by mass spectrometric identification[16,17] have led to the discovery of thousands of novel protein complexes,[18,19] although these studies are very incomplete, include mixed complexes, cover a very limited number of physiological states, and weakly bound subunits are underrepresented or absent. In parallel with these efforts, MS combined with chemical crosslinking (CXL) has become an increasingly important method for constraining protein structures and detecting interactions[20–23]. Improved CXL reagents have been developed with features that overcome many of the limitations previously associated with these experiments. Several crosslinkers have incorporated affinity tags for enrichment of crosslinked peptides[24,25], isotope encoding of crosslinkers allows recognition of modified peptides in the original MS scan[26–28], and MS cleavable crosslinkers facilitate identification of the peptide sequence via tandem MS[25,29–31]. MS can also be used to directly analyze the mass and stoichiometry of intact protein complexes using native-state nano-electrospray (nESI) coupled directly to tandem mass analyzers having a broad mass range[32,33]. When selected for collision induced dissociation (CID), such protein complex ions typically produce product ions bearing charge states that are asymmetric with respect to their

respective masses, with relatively unfolded highly-charged monomers being ejected from the precursor assembly leaving behind relatively compact charge-stripped oligomers[34,35]. In addition, ion mobility-mass spectrometry (IM-MS) can be brought to bear to record the mass and the collision cross-section (CCS) of an intact complex in a single experiment[36,37], along with the collision induced unfolding (CIU) of a protein complex ion that precedes CID[38,39]. Such IM-MS and MS/MS measurements are often integrated with other sources of structural information to build comprehensive models of intact multiprotein complexes that remain refractory to other, more narrow structural biology workflows[40,41].

In this report, we describe a novel combination of IM-MS and CXL aimed at providing structural information for labile assemblies that are not easily accessed by native-state IM-MS analysis alone. Bottom-up analysis of crosslinked proteins in conjunction with the IM-MS analysis of intact protein complexes has previously been used to ascertain the quaternary structure of multiprotein assemblies[42]. In addition, the collision induced dissociation (CID)[34,35], CCSs[43], and gas-phase chemical modification[44] of small model proteins and complexes has been studied using various MS and CXL technologies aimed at probing fundamental aspects of protein folding or the MS methods employed in their observation. The above studies have all highlighted the challenges surrounding the use of intact mass measurements for the assignment of protein complex stoichiometry, including the ability of the technique to detect transient complexes and the dominance of asymmetric protein unfolding and monomer ejection during CID[34,45].

Here, we report the IM-MS analysis of intact protein complexes following treatment with standard and custom CXL and tagging reagents in an effort to increase the information content of typical intact native protein analysis. We utilize bissulfosuccinimidyl suberate (BS3), 1,4-bis(4-((2,5-dioxopyrrolidin-1-yl)oxy)-4-oxobutyl)-1,4-diazabicyclo[2.2.2]octane-1,4-diium bromide (DC4)[29] and a DABCO tagging reagent that comprises half of the DC4 CXL agent (MTag). Both of the latter reagents bear two permanent charges through the incorporation of the DABCO ring, and we determine the influence of all three reagents on complex CCS, as well as CIU and CID pathways. In general, the addition of tagging or CXL reagents results in an increase in protein complex CCS of 5–10%, which we attribute directly to the addition of the modifiers to the protein complex surface through molecular modeling. Protein complexes modified with either charged crosslinkers or tags, but not those treated with neutral crosslinkers, exhibit enhanced stability in the gas phase relative to CIU, indicating the importance of charge mobility in the context of gas-phase protein unfolding. Conversely, the stability of modified complexes with respect to CID favored BS3 treated samples, as DC4 is an MS cleavable linker and MTag does not crosslink the assembly. Finally, we note that the crosslinked protein complexes exhibit altered CID product ions that more strongly favor sub-complex formation when compared with control samples. Overall, we discuss these results in the context of their potential impact on both IM-MS analyses of intact protein complexes as well as high-throughput structural biology efforts more broadly.

Materials and Methods

Materials

Triose phosphate isomerase (rabbit, TPI), avidin (chicken egg white, AVD), alcohol dehydrogenase (yeast, ADH), pyruvate kinase (rabbit muscle, PK), aldolase (rabbit muscle, ALD), transthyretin (human, TTR), Concanavalin A (jack bean, ConA), glutamate dehydrogenase (bovine liver, GDH) were purchased from Sigma Aldrich. A subset of these (TPI, AVD, ALD, TTR) were chosen for detailed IM-MS and CIU analysis, as they represent a broad cross-section of protein structures and stabilities. GDH was subjected to CXL treatment, but was not observed to undergo sufficient gas-phase unfolding following cross-linking, and thus not included in our CIU/CID analysis here. All other proteins listed were used for CCS calibration. Micro bio-spin columns with bio-gel P6 or P30 in a sodium chloride/citrate (SSC) buffer were purchased from Biorad.

Crosslinking, Tagging Reagents, and Sample Clean-up

BS3 was purchased from Fisher Scientific, and DC4 was synthesized as described previously[29]. A tagging reagent related to DC4 (MTag, structure shown in Figure 1A) was synthesized using a similar methodology (see Supplemental Information for details). Proteins were dissolved in 100 mM triethylammonium bicarbonate (TEAB) pH 7.0 to make 5 μg/μl (AVD – 64kDa, TTR – 56kDa, TPI – 53kDa), 10 μg/μl (ALD – 156kDa) or 15 μg/μl (GDH – 336kDa) solutions for chemical modification. Freshly prepared solutions of 100mM BS3, DC4, and M Tag in 100 mM TEAB, pH 7.0 were added in a 50–100 molar excess to the protein monomer and allowed to react for 30 minutes. Following modification, the proteins were desalted and buffer exchanged into 200mM ammonium acetate with a Biorad P30 microspin column according to manufacturer instructions. Prior to analysis, the crosslinked and tagged proteins were diluted to a final concentration of 20 μM with 200mM ammonium acetate.

Ion Mobility-Mass Spectrometry

A quadrupole ion mobility time-of-flight mass spectrometer (Synapt G2 HDMS, Waters, Milford, MA, USA) was used for all ion mobility experiments (see Supporting Information for instrument settings and conditions). To investigate the gas-phase stability of crosslinked protein complexes, ions were selected for CIU. For each protein, the ions selected for collisional activation were found at *m/z* values corresponding to the same charge state (14^+ TTR, 15^+ TPI, 17^+ AVD, 26^+ ALD) in the unmodified, crosslinked, and tagged samples. Collisional activation was achieved by increasing the trap collision voltage in 5V steps from 0–200V.

Data Analysis and Molecular Modeling

All mass spectra were analyzed using MassLynx 4.1 software and calibrated externally using a 100 mg/mL solution of cesium iodide. Spectra were smoothed using the mean of 100 channels twice, and no background correction steps were taken. For CCS measurements, PK, ADH, GDH, AVD, and TTR were used as calibrants via a previously published method, and carry an experimental error of 3%[37]. Analysis of ion intensities, fragmentation

pathways, and protein unfolding were accomplished as described previously (see Supporting Information for details)[46]. For purposes of comparison only, all trap collision voltages were converted to collision energy (eV) based on center of mass calculations described previously[47,48]. DC4 crosslinker models were manually constructed and docked onto the crystal structure of intact AVD tetramer (1AVE) using HEX 8.0.0[49]. Thirty identical DC4 molecules were randomly distributed on the outer surface of AVD tetramer with a nearest docking distance ranging from 2–4 Å, to mimic the crosslinking of lysine residues. The resultant models, together with the intact AVD structure, were further subjected to MOBCAL[50,51] and IMoS[52] theoretical CCS calculations (see Supporting Information for details).

Bottom-up Analysis of Chemical Cross Linking

A 5μg/μl solution of AVD in 100mM triethyl ammonium bicarbonate, pH 7.5 (TEAB) was combined with 10 mM DC4 prepared immediately before use in 100mM TEAB, pH 7.5 in a 50:1 molar ratio of crosslinker to AVD monomer. The mixture was allowed to react for 30 minutes at room temperature. Following this step, all samples were digested with cyanogen bromide in trifluoroacetic acid, followed by trypsin in ammonium bicarbonate, separated using an Agilent 1100 high performance liquid chromatography system, and mass analyzed using a 4800 MALDI TOF/TOF mass spectrometry platform (Applied Biosystems/Sciex). See the Supporting Information documentation for more information.

Results

Model homo-oligomers were crosslinked individually with BS3 and DC4 and then analyzed by MS (AVD in Figure 1A and all complexes in Figure S-1). A cursory examination of the data revealed that BS3-crosslinked proteins appeared to display similar average charge states to unmodified proteins, however the charge states for DC4-crosslinked and M-Tagged proteins shift to higher values. In all cases, MS peaks were resolved sufficiently to distinguish charge states; however, for all complexes studied MS/MS data were collected to ensure accurate mass measurements and assignments of charge states (Figure 1B). Similarly, shifts to higher masses were observed for all modified proteins – for each BS3 crosslink 180Da are added, BS3 dead-ends add 192Da, DC4 crosslinks add 250Da, DC4 dead-ends add 268Da and M-tags add 197Da each. Overall, BS3-crosslinked proteins exhibited a 6–8% increase in mass, DC4-crosslinked proteins 7–11%, and M Tagged proteins 8–12%. For the protein TPI, this would result in 20–32 molecules of crosslinker or tag added, TTR 21–31, AVD 27–34, ALD 55–67, and GDH 90–144. In all cases, these values are in good agreement with both the number of primary amines (lysine residues and the N-termini) within the complete sequences of our target protein complexes (TPI – 44, TTR – 36, AVD – 40, ALD – 108, GDH-198) and their solvent exposed lysine residues (TPI-42, TTR-28, AVD-36, ALD-100, GDH-156) based on available X-ray structures[53–57]. The addition of CXL molecules in excess of the number of available primary amines within the target sequence can be interpreted as evidence of reactions between the CXL agent NHS esters and other protein functional groups[58]. The CCSs of multiple crosslinked and tagged proteins were also measured (Figure 1C) and an increase of 5–10% in CCS was observed, regardless of

crosslinker or tag used, in a manner consistent with the observed mass increases discussed above.

For the data discussed above, the protein complexes analyzed were observed as compact structures, indicated by narrow IM drift time and charge state distributions similar to those observed under control conditions. To measure the stability of these structures, one charge state of each oligomer was isolated (14^+ TTR, 15^+ TPI, 17^+ AVD, 26^+ ALD), and collisionally activated by increasing an acceleration voltage that injects ions into the ion trap situated prior to the IM separator. As the collision energy was increased, a wider distribution of IM drift times was observed, indicating protein CIU[34,38]. In Figure 2A, the percentage of the compact, native-like structural family observed is shown as a function of collision energy for TTR, TPI, AVD, and ALD complexes. Compared to unmodified protein complexes (grey), BS3-crosslinked proteins (red) required similar collision energies to undergo CIU. However, proteins crosslinked (blue) or tagged (orange) with reagents containing charged quaternary amines exhibited increased resistance to CIU, with altered unfolding threshold energies that increased by ~23% on average.

In order to track the unfolding pathways adopted by modified and crosslinked protein complex ions, we created CIU fingerprints for selected charge states of the assemblies studied here. The CIU fingerprints of unmodified, BS3-crosslinked, DC4-crosslinked, and MTagged TTR (14^+), TPI (15^+), and AVD (17^+) are shown in Figure 2B. The BS3-crosslinked proteins have CIU fingerprints that possess many features in common with those recorded for unmodified control samples. For example, all three protein complexes shown in Figure 2B ultimately achieve unfolded structures that exhibit between 1.6 and 1.8 times larger CCS values at the largest collision energies probed when compared to those observed at lower energies in both BS3-treated and control samples. In addition, the collision energies required to initiate CIU remains unchanged for all three assemblies shown upon the addition of BS3. Specifically, the BS3-crosslinked AVD tetramer first undergoes CIU at a collision energy of ~0.35eV, a value that is nearly identical to that observed for the unmodified AVD tetramer. Similar trends are observed for TTR and TPI. Clear differences are also recorded between the CIU patterns adopted by BS3-modified complexes when compared to control samples. In general, BS3-treated assemblies adopt fewer defined intermediate structures during gas-phase unfolding when compared to complexes that have not undergone CXL treatment.

In contrast to BS3-linked protein complex ions, assemblies treated with either DC4 or MTag bear little resemblance to the CIU patterns recorded for control samples. In general, such assemblies require significantly higher collision energies to initiate unfolding, and have even fewer defined intermediates than those treated with BS3. For example, the CIU threshold energy for TTR increases by ~38% (from 0.32 to 0.44 eV) upon the addition of DC4 crosslinkers. Similar increases in stability are observed upon the addition of MTag, and across all three protein complexes upon the addition of any covalent modification that bears permanent charge. In further contrast to BS3-treated protein complexes, those having undergone reactions with DC4 and MTag reagents produce protein complexes that exhibit substantially decreased ultimate CCS values at high energies. On average, the largest CCSs achieved for DC4 linked protein complexes are decreased 9% relative to control, and those

treated with MTag are decreased by 6%. Differences between these most-unfolded structures achieved upon activating DC4 and MTag treated assemblies can, however, be detected in some cases. For example, the ultimate CCS achieved at high energies for MTagged TTR is 59 nm^2, which is a value nearly identical to control and significantly different from those recorded for DC4-crosslinked samples under similar conditions (60 nm^2). Overall, this effect results in a dramatically-decreased slope in the CIU data for complexes treated with charged CXL agents when compared with control data, further indicative of their increased CIU stabilities achieved in these cases when compared to BS3-treated samples.

In order to probe the CID of CXL-modified and tagged protein complexes, we monitored the m/z of product ions generated at energies beyond the CIU thresholds discussed above (Figure 3A, B). In general, the addition of CXL agents increased the collision energies required to initiate CID of modified intact complexes. In contrast, those assemblies having undergone labeling reactions with the MTag reagent required only modestly increased collision energies to undergo CID. BS3-treated samples exhibited the greatest amount of CID stability, followed by those treated with DC4 in general. For example, at maximized collision energies, only 70% of BS3-crosslinked AVD undergoes CID, whereas unmodified AVD exhibits complete dissociation at 33% of this energy. DC4 addition, overall, confers less stability to protein complex ions relative to dissociation than BS3 in all cases save TPI, an observation that agrees with the MS-cleavability of DC4 observed in bottom-up sequencing experiments[29].

Through a detailed analysis of CID product ion populations, we have detected evidence of altered fragmentation pathways when precursor ions having undergone CXL or chemical tagging are selected for activation in comparison with control samples (Figures 3C, D). As expected, precursor ions treated with CXL agents exhibited enhanced populations of protein subcomplexes reflective of inter-chain covalent links that survive the CID process. For example, while no dimer product ions are observed upon CID of unmodified AVD (Figure 3C and S2), both DC4 and BS3-treated samples generate ion populations where ~25% of the total integrated product ion intensity is dimeric. While we observe that CID of unmodified TTR produces some dimer ion signal (~6% of recorded signal intensity) as observed previously[38], these signals are significantly enhanced upon both BS3 and DC4 modification, resulting in dimer signal increases of ~16 and 6% relative to control respectively. Substantially smaller increases in dimer ion intensities are observed for MTagged ions following CID, resulting in increases of dimeric product ion signal of~2 and 4% for AVD and TTR respectively.

Further evidence of altered CID pathways for chemically modified protein complexes can be observed in Figure 3D, which tracks the relative charge states of the precursor ions produced, and is thus a sensitive probe for the level of CIU undergone by the assembly prior to product ion formation[59,60]. For example, the average charge states of the monomer ions produced upon the collisional activation of tetrameric AVD and TTR were examined in order to evaluate the charge asymmetry for CID products generated from chemically linked and labeled precursor ions. In the case of AVD, 16^+ precursor ions generated by nESI under control conditions produce both trimer and monomer product ion populations upon CID, each having an average charge state of approximately 8^+. However, following CXL with

BS3 or DC4, we observe that modified 16^+ AVD precursor ions generate trimer ions having an increased average charge state of 10^+, and a decreased average monomer charge state of 6^+, thus resulting in a 62% and 38% share of the precursor ion charge respectively (Figure 3D). These values are considerably closer to the charge partitioning expected based on the masses of the product ions alone (75% and 25%), as well as the relative proportions expected based on their folded relative surface areas (70–75% and 25–30%, depending upon the coordinate files used, see Supplemental Information). A similar effect is observed for CXL-modified 14^+ TTR precursor ions, for which trimer product ions retain 60% of the precursor charge and the monomers 40%. TTR and AVD samples treated with MTagged produced less-consistent alterations in charge partitioning when compared with CXL treated assemblies. AVD tetramers produced product ion populations similar to control, while the CID products of MTagged TTR exhibited similar charge partitioning to CXL treated complexes.

In order to extract additional data supporting the relative compactness of product ions produced from CID of CXL-treated protein complexes, we analyzed CCS values recorded for the CID product ions generated in the experiments described above (Figures 3E, F). In the case of AVD, BS3-crosslinked dissociated subunits (red) are similar in size when compared to unmodified monomers (grey) and are within error of the calculated CCS values (dashed line) expected for both the AVD monomer and trimer. In contrast, DC4-crosslinked and MTagged AVD monomers and trimers appear significantly larger than the unmodified and BS3-crosslinked product ions. Multiple CCS populations are observed for unmodified TTR monomers as a function of charge state, however no such differences in CCS are observed in CXL-treated or MTagged TTR monomers. Furthermore, TTR treated with DC4 produces trimer product ions having significantly larger CCS values than those observed for the unmodified complex, BS3-crosslinked, or MTagged trimers which are all observed to have approximately identical CCS values. In general, we observe strong CCS and MS data supporting significant and differential influences of CXL and tagging agents on product ion conformations.

Increases in both protein complex intact mass and CCS were observed upon treatment with CXL and tagging agents. In order to verify that these increases are associated primarily with covalent chemical modification and cross-linking, we undertook both a bottom-up analysis of tryptic peptides produced from CXL-treated complexes, as well as molecular modeling experiments aimed at assessing the impact of CXL agents alone on protein complex CCS values. For example, Figure 4A shows a color coded X-ray analysis of the 36 available lysine residues on the surface of the AVD tetramer (PDB code AVD1). When we subjected DC4-treated AVD tetramers to bottom-up MS analysis, we observed 6 lysine modifications (Figure 4B), representative of both inter- and intra-chain cross-links, having distances ranging from 8.9Å to 34.1Å (Table S-1), in line with previous reports.[29] Furthermore, these data are in strong agreement with denaturing gels acquired across the multiple protein complexes studied in this report (Figure S3). In order to investigate the origin of the CCS increases observed in our IM-MS data upon treatment with CXL and tagging agents, we created a series of AVD tetramer models having DC4 molecules (our largest CXL agent) docked to its surface. For example, when 30 molecules of DC4 are docked to the surface of the AVD tetramer, a value consistent with the increases observed in intact protein complex

mass upon CXL treatment (Figure 1A), we compute an 8.5% increase in CCS when CXL-modified AVD models are compared with unmodified AVD models. This value is similar to our experimentally-determined CCS differences observed in Figure 1C (5–10% CCS increase), thus providing a plausible mechanism for our IM-MS results shown in Figure 1B.

Discussion

General Features of Chemically-modified Protein Complex Ions

All protein complexes treated with tags or CXL agents exhibited monomodal yet broadened MS distributions, as well as monomodal CCS distributions (Figure 1 and S-1), the magnitudes of which appear to be relatively independent of the agent utilized and are similar to those observed upon the adduction of non-volatile counter-ions in nESI solutions.[46,48] In addition, we observe that the charge state distributions for chemically modified protein complexes are, in general, altered in a manner dependent upon the modification agent used. For example, BS3-crosslinked proteins maintain a similar charge state distribution to protein complex ions created under control nESI conditions, despite the reduction in the number of available primary amines on the protein surface following the BS3 crosslinking reaction. In contrast, both DC4 and MTag modified proteins shifted to higher average charge states, apparently due to replacement of the primary amine by a charged quaternary amine. These observations are congruent with our current understanding of protein complex ion formation mechanisms in nESI, where charging is largely dictated by available protein ion surface area and charge-bearing tags result in pre-formed ions that result in a mild supercharging effect.[61]

Fixed Charges Stabilize Protein Structure in vacuo

CIU and CID data shown in Figures 2 and 3 illustrate clear differences between the gas-phase stabilities of BS3-treated complexes, and those having undergone reactions with either MTag or DC4. In general, complexes treated with BS3 exhibit similar CIU properties to unmodified complexes, but enhanced CID stabilities. In contrast, DC4 treated and MTagged assemblies exhibit enhanced CIU stabilities and CID stabilities similar to control complexes. A comparison of BS3 and DC4 structures reveals three key differences between these agents: length, CID cleavability, and charge. BS3 is an 11.4 Å crosslinker with a neutral alkane chain spacer region, whereas DC4 is both longer (18 Å) and doubly charged. The MTag results shown in Figures 2 and 3 where no lysine-lysine links are possible, strongly indicates that the addition of permanent charge is the key driver for the CIU and CID stabilities observed in our IM-MS dataset, rather than the length of the compounds used. This conclusion is supported by our current mechanistic understanding of the collisional activation process for protein complex ions, which requires mobile charges to create collisionally-unfolded intermediate forms of the protein prior to CID.[34,35] The addition of DC4, MTag or similar linkers to the protein complex creates a large population of non-mobile charges on the protein surface, likely frustrating this CIU mechanism. Similarly, since DC4 is CID cleavable,[29] it provides a lesser increase in CID stability in most cases than BS3, which forms covalent bonds with strengths similar to the peptide backbone. Data for TPI shows a CID stability trend opposite to the general case described above, and we interpret such results as evidence of incomplete TPI BS3 crosslinking for the samples and conditions used in this study. Similarly, minor amounts of unmodified protein within DC4

and BS3 ion pools is a likely causal factor in some of the detailed trends observed in Figure 3a, where clear evidence of multimodal CID trends are evident.

Chemical Modification Alters the Dissociation Pathways of Protein Complex Ions

The differences described above, surrounding the CIU and CID stabilities of chemically modified protein complexes when compared with unmodified assemblies, links clearly to the product ion populations created for each of these classes of complex ions upon collisional activation. Figure 3 clearly illustrates that complexes treated with CXL agents and MTag produce a significantly greater amount of product ions related to sub-complexes, rather than the unfolded monomers and charge reduced, stripped oligomers typically observed in such experiments, indicating a shift in the operative CID mechanism for chemically-modified protein complexes. This mechanistic shift likely results from both additional covalent links generated both within and between subunits in the complexes treated with CXL agents, as well as the non-mobile charges installed through MTag and DC4 treatment, although not to equal extents. The addition of covalent bonds within the structures of AVD and TTR, for example, appear to more strongly influence their CID thresholds, as well as increase the dimer ion intensities observed following CID, when compared to those complexes with addition of non-mobile charges solely through MTag treatment. Inter-molecular crosslinking can readily be used to rationalize the observation of strong dimer CID product ion signals from intact tetramer ions, particularly as, upon increased dissociation, marker ions indicative of crosslinker cleavage are observed (Figure S4). In addition, increased intra-molecular crosslinks likely increase the rigidity of individual subunits, thus limiting their unfolding. Such altered product ions can be observed in charge-enhanced protein complex ions, where general trends in subcomplex product ion production are often linked to enhanced subunit stability values[62], and are also commonly observed in surface induced dissociation (SID) data where high-energy single collision events allow complex ions to access dissociative transitions that do not necessarily rely upon the unfolding of individual subunits.[63,64] We also observe increased CCS values for both monomers and trimers produced from the CID of both CXL-treated and MTagged complexes, indicating that both charge mobility and the addition of covalent links have some influence on product ion structure. Although the differences observed for MTagged complexes, where charge mobility effects on the data are isolated, are clearly smaller than those cases where CXL agents are used, and the shorter, more stable links created by BS3 appear to produce the largest product ions on average, all three classes of the modified complexes studied here produce significant changes in product ion CCS across all charge states. Charge reduced protein complexes, when selected as precursor ions for CID, have been observed to produce product ions of similarly altered size, and it is likely that chemical modification of protein complexes extends these general benefits to higher charge state protein complexes.[65,66] Overall, chemical modification appears to be a promising route to the alteration of the typical protein complex CID mechanism, resulting in increased signals for subcomplex product ions and larger CCS values for both monomers and trimers reflective of lessened gas-phase collapse, both of which mirror SID and charge-altered CID datasets that have proven useful for structural biology.[67,68]

Conclusions

Stabilization of protein complexes for gas phase analysis is necessary for effective analysis of structures by native IM-MS. Fragile complexes are often unfolded or dissociated during ionization and transfer into the mass spectrometer resulting in loss of key structural information. Developing conditions that stabilize structures allows IM-MS to be applied to the analysis of fragile complexes, as well as measurements of more accurate CCSs and intact masses, both of which are critical for the development of multiprotein models. Subsequent dissociation is also a key component in determining the identity and connectivity of proteins in a complex. MS cleavable crosslinkers, such as DC4, which act to both stabilize protein complex structures in the gas phase and dissociate with the addition of higher collision energies, appears to be a promising route toward the facile identification of the complex subunits and subcomplexes. Although BS3-crosslinked complexes can also maintain such interactions in the gas phase, those complexes require much higher energy to dissociate and do not provide the same level of stability enhancement to the protein structure in the gas-phase. While we interpret our IM and MS data based primarily upon the identity of the CXL agent employed for chemical modification, it should be noted that the extent of the chemical modification generated by the linkers used will also require future optimization. In addition, we observe size increases of 5–10%, on average, for chemically-modified complexes. Such size changes, if they were completely unknown, could significantly influence using CCS data to build protein models. The data shown in this work, as well as future data collected for a larger number of model systems, will allow for estimates of such size increases to be normalized during structural modeling.

The alternative fragmentation pathways observed with crosslinked complexes have significant implications for IM-MS and for native MS applications. Additional CID data can potentially be collected on complexes that have to date been inaccessible due to the asymmetric distribution of charge after fragmentation. Clearly, there are challenges associated with the continued development of the IM-MS strategies outlined here. The broadened distribution of molecular masses created upon CXL treatment clearly degrades the ability of IM-MS to detect protein isoforms and ligand bound states within the targeted complexes, and may also obscure the protein composition captured in discovery-mode experiments. In the future, similar CXL or tagging agents, optimize to minimize the resultant mass distributions and combined with bottom-up proteomics data, will likely form the foundation of a comprehensive method that enables the acquisition of accurate CCSs and masses of fragile complexes, identities of interacting proteins, and sites of interactions which are each crucial components for building accurate models of protein complexes across the entirety of the proteome.

Supplementary Material

Refer to Web version on PubMed Central for supplementary material.

Acknowledgments

The authors acknowledge support from the National Institutes of Health (National Institute of General Medical Sciences, 1R01GM095832 to BTR and PCA) which supports technology development for high-throughput

structural biology research at UM. In addition, this work was supported by an M-cubed grant from the University of Michigan (BTR and PCA).

References

1. Alberts B. Cell. 1998; 92:291–294. [PubMed: 9476889]
2. Shen H-B, Chou K-C. J. Proteome Res. 2009; 8:1577–1584. [PubMed: 19226167]
3. Hart GT, Lee I, Marcotte ER. Bmc Bioinformatics. 2007; 8:236. [PubMed: 17605818]
4. Hartwell LH, Hopfield JJ, Leibler S, Murray AW. Nature. 1999; 402:C47–C52. [PubMed: 10591225]
5. Han J-DJ, Bertin N, Hao T, Goldberg DS, Berriz GF, Zhang LV, Dupuy D, Walhout AJM, Cusick ME, Roth FP, Vidal M. Nature. 2004; 430:88–93. [PubMed: 15190252]
6. Alber F, Dokudovskaya S, Veenhoff LM, Zhang W, Kipper J, Devos D, Suprapto A, Karni-Schmidt O, Williams R, Chait BT, Rout MP, Sali A. Nature. 2007; 450:683–694. [PubMed: 18046405]
7. Taverner T, Hernández H, Sharon M, Ruotolo BT, Matak-Vinković D, Devos D, Russell RB, Robinson CV. Acc. Chem. Res. 2008; 41:617–627. [PubMed: 18314965]
8. Blackstock WP, Weir MP. Trends Biotechnol. 1999; 17:121–127. [PubMed: 10189717]
9. Peng J, Elias JE, Thoreen CC, Licklider LJ, Gygi SP. J. Proteome Res. 2003; 2:43–50. [PubMed: 12643542]
10. Wilm M, Shevchenko A, Houthaeve T, Breit S, Schweigerer L, Fotsis T, Mann M. Nature. 1996; 379:466–469. [PubMed: 8559255]
11. Washburn MP, Wolters D, Yates JR. Nat. Biotechnol. 2001; 19:242–247. [PubMed: 11231557]
12. Wolters DA, Washburn MP, Yates JR. Anal. Chem. 2001; 73:5683–5690. [PubMed: 11774908]
13. Cantin GT, Yi W, Lu BW, Park SK, Xu T, Lee JD, Yates JR. J. Proteome Res. 2008; 7:1346–1351. [PubMed: 18220336]
14. Omenn GS, States DJ, Adamski M, Blackwell TW, Menon R, Hermjakob H, Apweiler R, Haab BB, Simpson RJ, Eddes JS, Kapp EA, Moritz RL, Chan DW, Rai AJ, Admon A, Aebersold R, Eng J, Hancock WS, Hefta SA, Meyer H, Paik YK, Yoo JS, Ping PP, Pounds J, Adkins J, Qian XH, Wang R, Wasinger V, Wu CY, Zhao XH, Zeng R, Archakov A, Tsugita A, Beer I, Pandey A, Pisano M, Andrews P, Tammen H, Speicher DW, Hanash SM. Proteomics. 2005; 5:3226–3245. [PubMed: 16104056]
15. Wilhelm M, Schlegl J, Hahne H, Gholami AM, Lieberenz M, Savitski MM, Ziegler E, Butzmann L, Gessulat S, Marx H, Mathieson T, Lemeer S, Schnatbaum K, Reimer U, Wenschuh H, Mollenhauer M, Slotta-Huspenina J, Boese J-H, Bantscheff M, Gerstmair A, Faerber F, Kuster B. Nature. 2014; 509:582–587. [PubMed: 24870543]
16. Verhagen AM, Ekert PG, Pakusch M, Silke J, Connolly LM, Reid GE, Moritz RL, Simpson RJ, Vaux DL. Cell. 2000; 102:43–53. [PubMed: 10929712]
17. Li YQ, Ren J, Yu WH, Li Q, Kuwahara H, Yin L, Carraway KL, Kufe D. J. Biol. Chem. 2001; 276:35239–35242. [PubMed: 11483589]
18. Gavin AC, Bosche M, Krause R, Grandi P, Marzioch M, Bauer A, Schultz J, Rick JM, Michon AM, Cruciat CM, Remor M, Hofert C, Schelder M, Brajenovic M, Ruffner H, Merino A, Klein K, Hudak M, Dickson D, Rudi T, Gnau V, Bauch A, Bastuck S, Huhse B, Leutwein C, Heurtier MA, Copley RR, Edelmann A, Querfurth E, Rybin V, Drewes G, Raida M, Bouwmeester T, Bork P, Seraphin B, Kuster B, Neubauer G, Superti-Furga G. Nature. 2002; 415:141–147. [PubMed: 11805826]
19. Ho Y, Gruhler a, Heilbut A, Bader GD, Moore L, Adams SL, Millar A, Taylor P, Bennett K, Boutillier K, Yang L, Wolting C, Donaldson I, Schandorff S, Shewnarane J, Vo M, Taggart J, Goudreault M, Muskat B, Alfarano C, Dewar D, Lin Z, Michalickova K, Willems AR, Sassi H, Nielsen PA, Ramuseen KJ, Andersen JR, Johansen LE, Hensen LH, Jespersen H, Podtelejnikov A, Nielsen E, Crawford J, Poulsen V, Sorensen BD, Matthisen J, Hendrickson RC, Gleeson F, Pawson T, Moran MF, Durocher D, Mann M, Hogue CW, Figeys D, Tyers M. Nature. 2002; 415:180–183. [PubMed: 11805837]
20. Tang X, Yi W, Munske GR, Adhikari DP, Zakharova NL, Bruce JE. J. Proteome Res. 2006; 6:724–734.

21. Sinz A. Anal. Bioanal. Chem. 2010; 397:3433–3440. [PubMed: 20076950]
22. Liu F, Rijkers DTS, Post H, Heck AJR. Nat Meth. 2015; 12:1179–1184.
23. Ding Y, Fan S, Li S, Feng B, Gao N, Ye K, He S-M, Dong M-Q. Anal. Chem. 2016
24. Chowdhury SM, Du X, Tolic N, Wu S, Moore RJ, Mayer MU, Smith RD, Adkins JN. Anal. Chem. 2009; 81:5524–5532. [PubMed: 19496583]
25. Petrotchenko EV, Serpa JJ, Borchers CH. Mol. Cell. Proteomics. 2011:10.
26. Seebacher J, Mallick P, Zhang N, Eddes JS, Aebersold R, Gelb MH. J. Proteome Res. 2006; 9:2770–2282.
27. Ihling CH, Schmidt A, Kalkhof S, Schultz D, Stingl C, Mechtler K, Haack M, Beck-Sickinger A, Cooper D, Sinz A. J. Am. Soc. Mass. Spectrom. 2006; 17:1100–1113. [PubMed: 16750914]
28. Merkley ED, Baker ES, Crowell KL, Orton DJ, Taverner T, Ansong C, Ibrahim YM, Burnet MC, Cort JR, Anderson GA, Smith RD, Adkins JN. J. Am. Soc. Mass. Spectrom. 2013; 24:444–449. [PubMed: 23423792]
29. Clifford-Nunn B, Showalter HDH, Andrews P. J. Am. Soc. Mass. Spectrom. 2012; 23:201–212. [PubMed: 22131227]
30. Hoopmann MR, Weisbrod CR, Bruce JE. J. Proteome Res. 2010; 9:6323–6333. [PubMed: 20886857]
31. Muller MQ, Dreiocker F, Ihling CH, Schafer M, Sinz A. Anal. Chem. 2010; 82:6958–6968. [PubMed: 20704385]
32. Kennaway CK, Benesch JLP, Gohlke U, Wang L, Robinson CV, Orlova EV, Saibi HR, Keep NH. J. Biol. Chem. 2005; 280:33419–33425. [PubMed: 16046399]
33. Benesch JL, Aquilina JA, Ruotolo BT, Sobott F, Robinson CV. Chem. Biol. 2006; 13:597–605. [PubMed: 16793517]
34. Jurchen JC, Williams ER. J. Am. Chem. Soc. 2003; 125:2817–2826. [PubMed: 12603172]
35. Jurchen JC, Garcia DE, Williams ER. J. Am. Soc. Mass. Spectrom. 2004; 15:1408–1415. [PubMed: 15465353]
36. Ruotolo B, Benesch JLP, Sandercock AM, Hyung SJ, Robinson CV. Nat. Protoc. 2008; 3:1139–1152. [PubMed: 18600219]
37. Bush MF, Hall Z, Giles K, Hoyes J, Robinson CV, Ruotolo BT. Anal. Chem. 2010; 82:9557–9565. [PubMed: 20979392]
38. Ruotolo BT, Hyung S-J, Robinson PM, Giles K, Bateman RH, Robinson CV. Angew. Chem. Int. Ed. 2007; 46:8001–8004.
39. Benesch JLP. J. Am. Soc. Mass. Spectrom. 2009; 20:341–348. [PubMed: 19110440]
40. Rostom AA, Sunde M, Richardson SJ, Schreiber G, Jarvis S, Bateman R, Dobson CM, Robinson CV. Proteins. 1998; (Suppl 2):3–11.
41. Rostom AA, Fucini P, Benjamin DR, Juenemann R, Nierhaus KH, Hartl FU, Dobson CM, Robinson CV. Proc Natl Acad Sci U S A. 2000; 97:5185–5190. [PubMed: 10805779]
42. Motshwene PG, Moncrieffe MC, Grossmann JG, Kao C, Ayaluru M, Sandercock AM, Robinson CV, Latz E, Gay NJ. J. Biol. Chem. 2009; 284:25404–25411. [PubMed: 19592493]
43. Smith DP, Giles K, Bateman RH, Radford SE, Ashcroft AE. J. Am. Soc. Mass. Spectrom. 2007; 18:2180–2190. [PubMed: 17964800]
44. Webb I, Mentinova M, McGee W, McLuckey S. J. Am. Soc. Mass. Spectrom. 2013; 24:733–743. [PubMed: 23463545]
45. Beardsley RL, Jones CM, Galhena AS, Wysocki VH. Anal. Chem. 2009; 81:1347–1356. [PubMed: 19140748]
46. Han L, Hyung S-J, Ruotolo BT. Faraday Discuss. 2013; 160:371–388. [PubMed: 23795511]
47. Shukla AK, Futrell JH. J Mass Spectrom. 2000; 35:1069–1090. [PubMed: 11006601]
48. Han L, Hyung S-J, Mayers JJS, Ruotolo BT. J. Am. Chem. Soc. 2011; 133:11358–11367. [PubMed: 21675748]
49. Macindoe G, Mavridis L, Venkatraman V, Devignes M-D, Ritchie DW. Nucleic Acids Res. 2010; 38:W445–W449. [PubMed: 20444869]

50. Mesleh MF, Hunter JM, Shvartsburg AA, Schatz GC, Jarrold MF. J. Phys. Chem. 1996; 100:16082–16086.
51. Shvartsburg AA, Jarrold MF. Chem. Phys. Lett. 1996; 261:86–91.
52. Larriba C, Hogan CJ. J. Phys. Chem. A. 2013; 117:3887–3901. [PubMed: 23488939]
53. Banerjee S, Schmidt T, Fang J, Stanley CA, Smith TJ. Biochemistry. 2003; 42:3446–3456. [PubMed: 12653548]
54. Sygusch J, Beaudry D, Allaire M. Biochemistry. 1987; 84:7846–7850.
55. Pugliese L, Malcovati M, Coda A, Bolognesi M. J Mol Biol. 1994; 235:42–46. [PubMed: 8289264]
56. Yokoyama T, Kosaka Y, Mizuguchi M. J Med Chem. 2014; 57:1090–1096. [PubMed: 24422526]
57. Aparicio R, Ferreira ST, Polikarpov I. J Mol Biol. 2003; 334:1023–1041. [PubMed: 14643664]
58. Madler S, Bich C, Touboul D, Zenobi R. J. Mass Spectrom. 2009; 44:694–706. [PubMed: 19132714]
59. Chowdhury SK, Katta V, Chait BT. J. Am. Chem. Soc. 1990; 112:9012–9013.
60. Dobo A, Kaltashov IA. Anal. Chem. 2001; 73:4763–4773. [PubMed: 11681449]
61. Kaltashov IA, Mohimen A. Anal. Chem. 2005; 77:5370–5379. [PubMed: 16097782]
62. A Loo J, A Benchaar S, Zhang J. Mass Spectrom. 2013; 2:S0013.
63. Jones CM, Beardsley RL, Galhena AS, Dagan S, Cheng G, Wysocki VH. J. Am. Chem. Soc. 2006; 128:15044–15045. [PubMed: 17117828]
64. Galhena AS, Dagan S, Jones CM, Beardsley RL, Wysocki VH. Anal. Chem. 2008; 80:1425–1436. [PubMed: 18247517]
65. Pagel K, Hyung S-J, Ruotolo BT, Robinson CV. Anal. Chem. 2010; 82:5363–5372. [PubMed: 20481443]
66. Bornschein RE, Ruotolo BT. Analyst. 2015; 140:7020–7029. [PubMed: 26331159]
67. Song Y, Nelp MT, Bandarian V, Wysocki VH. ACS Central Science. 2015; 1:477–487. [PubMed: 26744735]
68. Mehmood S, Marcoux J, Hopper JTS, Allison TM, Liko I, Borysik AJ, Robinson CV. J. Am. Chem. Soc. 2014; 136:17010–17012. [PubMed: 25402655]

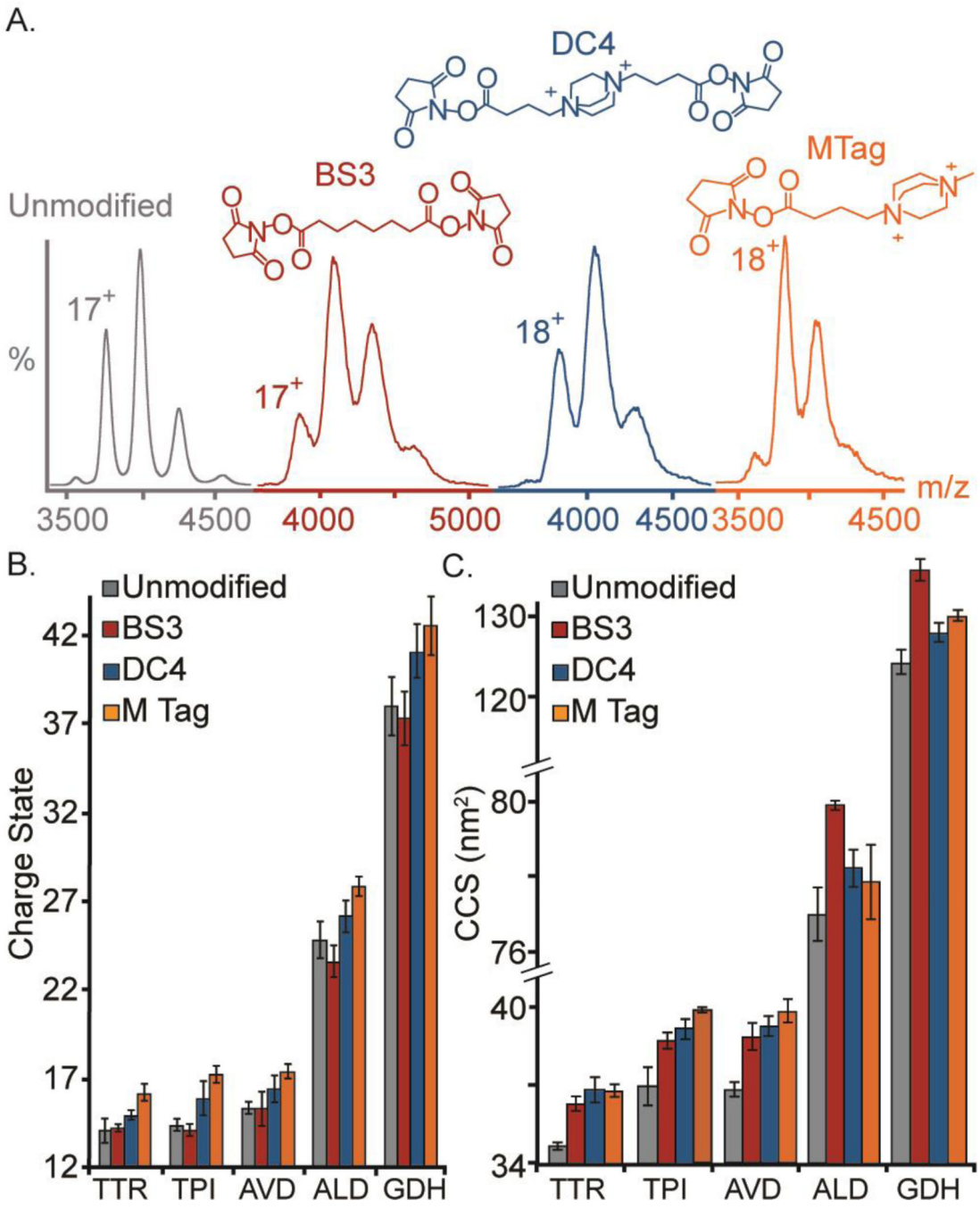

Figure 1. IM-MS of Intact Crosslinked Proteins

(A) Mass spectra of AVD unmodified (grey), BS3-crosslinked (red), DC4-crosslinked (blue), and MTagged (orange) are shown below the color-coded chemical structures of each chemical agent used in this study. (B) After crosslinking or tagging, the CCS of the intact protein complexes increases by 5–10%, as shown in the histogram shown, which plots ion CCS against the four forms of each complex studied. (C) A histogram plotting the average charge state recorded versus the chemically modified forms of each of the complex studied here reveals no differences in average charge state for BS3-crosslinked proteins, and

modestly-increased charge states for those proteins modified with a quaternary bearing chemical tags and CXL agents.

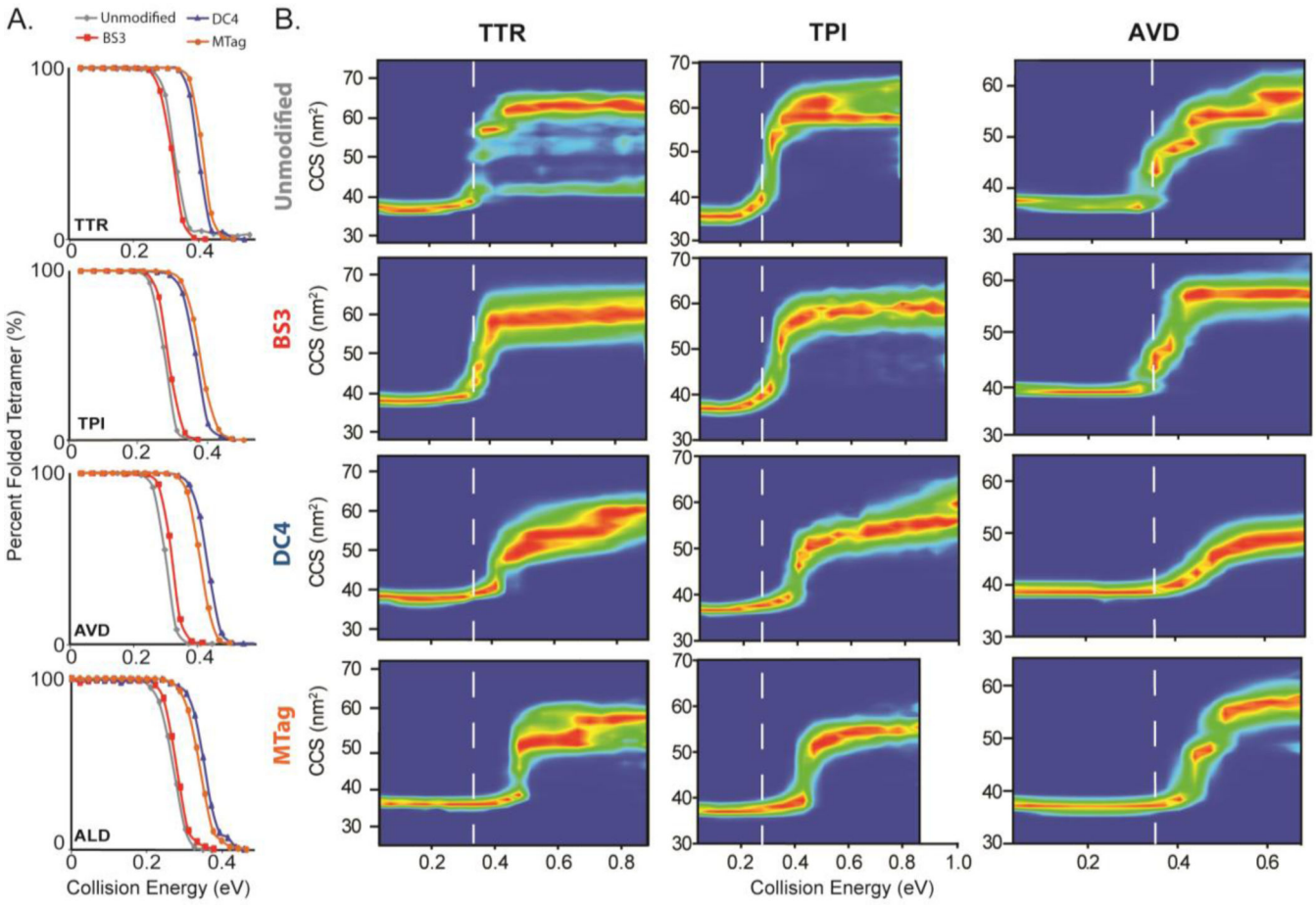

Figure 2. Collision Induced Unfolding of Crosslinked and Tagged Proteins

(A) Plots of the fractions of the observed compact forms of the protein complexes indicated against the collision energy used to activate the protein complexes (14^+ TTR, 15^+ TPI, 17^+ AVD, 26^+ ALD) show that clear differences in CIU transition energies are only observed for complexes having undergone reactions with chemical agents bearing permanent charge. (B) Complete CIU fingerprint data, plotting the CCSs of the isolated protein complexes against the collision energy used to activate the complex for each indicated protein complex form. Ion intensity is represented by color from blue (no signal) to red (most intense). The white dashed line is added to guide the eye, and reveals marked differences between the DC4 and MTag modified complexes when compared with both BS3 and unmodified proteins.

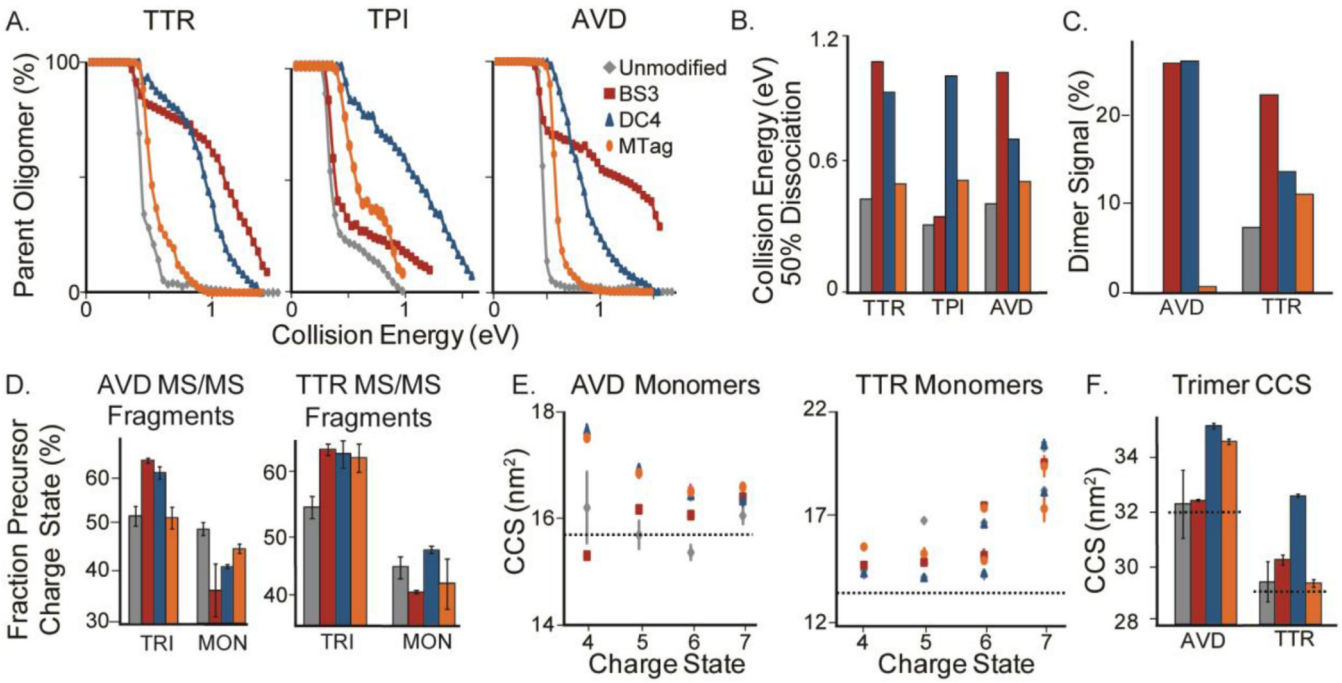

Figure 3. Collision Induced Dissociation of Modified Complexes

(A) Three plots of the fractional amount of intact protein oligomer observed by MS versus collision energy used for ion activation for the indicated protein complexes. As the collision energy is increased, the oligomeric proteins dissociate, however, once the proteins are crosslinked or tagged, higher energy is required for dissociation. (B) A histogram showing the energy value required to deplete the indicated intact protein complexes studied here by 50% of the original intensity. (C) A histogram plotting the percent of the total recorded ion signal corresponding to dimer product ion formation following CID for both AVD and TTR chemically modified forms as indicated. After crosslinking or tagging, the amount of dimer dissociated from the tetrameric complexes is higher than the unmodified tetramer, indicating dissociation through an alternate CID pathway. (D) Histograms showing the fractional percentage of the indicated tetrameric precursor ion charge carried away by either monomeric or trimeric product ions. After crosslinking, a more symmetric distribution of charge is observed between the trimer and monomer fragments. (E) Two plots showing monomer CCSs produced upon dissociation against their charge states for both AVD and TTR. A dashed line is used to indicate the theoretical CCS values expected for these ions based on X-ray data. Unmodified proteins are shown in grey, BS3-crosslinked proteins in red, DC4-crosslinked proteins in blue, and MTagged proteins are in orange throughout the figure. (F) A histogram showing trimer CCS values against the various modified forms of the tetramer precursor ions isolated for CID experiments. A dashed line is used to indicate the theoretical CCS values expected for these ions based on X-ray data.

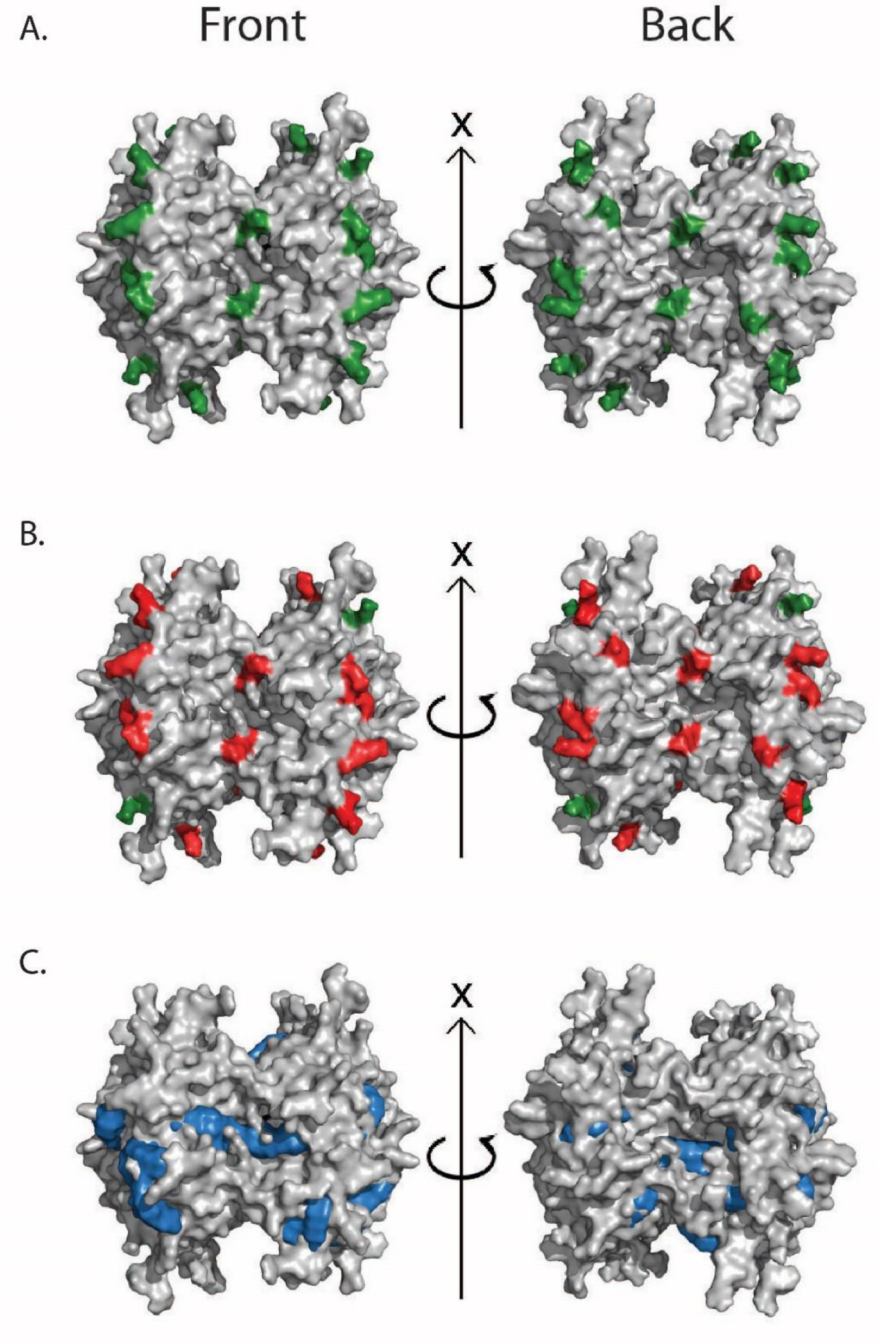

Figure 4. Molecular Modeling and Bottom-up Proteomics of CXL-treated AVD

(A) A surface fill projection of the AVD X-ray structure (PDBID: AVD1), with all surface-accessible lysine residues colored green. (B) The same surface projection, with overlaid red-colored lysine residues indicated all those observed to be modified and/or cross-linked during bottom-up proteomics experiments. (C) A surface projection of an example molecular model built to mimic CXL AVD samples. These models exhibit an increase in

CCS of 8.5% on average, in agreement with our experimental measurements (5–10% CCS increase).